The effect of pCO_2 on carbon acquisition and intracellular assimilation in four marine diatoms

Scarlett Trimborn *, Dieter Wolf-Gladrow, Klaus-Uwe Richter, Björn Rost

Alfred Wegener Institute for Polar and Marine Research, Am Handelshafen 12, 27570 Bremerhaven, Germany

ARTICLE INFO

ABSTRACT

The effect of pCO_2 on carbon acquisition and intracellular assimilation was investigated in the three bloom-forming diatom species, *Eucampia zodiacus* (Ehrenberg), *Skeletonema costatum* (Greville) Cleve, *Thalassionema nitzschioides* (Grunow) Mereschkowsky and the non-bloom-forming *Thalassiosira pseudonana* (Hust.) Hasle and Heimdal. *In vivo* activities of carbonic anhydrase (CA), photosynthetic O_2 evolution, CO_2 and HCO_3^- uptake rates were measured by membrane-inlet mass spectrometry (MIMS) in cells acclimated to pCO_2 levels of 370 and 800 µatm. To investigate whether the cells operate a C_4-like pathway, activities of ribulose-1,5-bisphosphate carboxylase (RubisCO) and phosphoenolpyruvate carboxylase (PEPC) were measured at the mentioned pCO_2 levels and a lower pCO_2 level of 50 µatm. In the bloom-forming species, extracellular CA activities strongly increased with decreasing CO_2 supply while constantly low activities were obtained for *T. pseudonana*. Half-saturation concentrations ($K_{1/2}$) for photosynthetic O_2 evolution decreased with decreasing CO_2 supply in the two bloom-forming species *S. costatum* and *T. nitzschioides*, but not in *T. pseudonana* and *E. zodiacus*. With the exception of *S. costatum*, maximum rates (V_{max}) of photosynthesis remained constant in all investigated diatom species. Independent of the pCO_2 level, PEPC activities were significantly lower than those for RubisCO, averaging generally less than 3%. All examined diatom species operate highly efficient CCMs under ambient and high pCO_2, but differ strongly in the degree of regulation of individual components of the CCM such as C_i uptake kinetics and extracellular CA activities. The present data do not suggest C_4 metabolism in the investigated species.

© 2009 Elsevier B.V. All rights reserved.

1. Introduction

Diatoms are a diverse and ecologically very important group contributing up to 40% of the oceans primary production (Nelson et al., 1995). Among the large diversity in this group, bloom-forming diatoms play a major role in determining the downward transport of organic carbon from surface waters to the deep ocean (Buesseler, 1998). Numerous diatom species are known to bloom frequently along continental margins and in upwelling regions where the nutrient availability is high (Smetacek, 1999). The occurrence of high diatom abundances in nutrient-rich waters has been related to several physiological adaptations. Mostly centric diatoms have evolved a vacuole that allows accumulating nutrients in excess of its immediate growth requirements and therewith deprives competing taxa of these essential resources (Raven, 1997; Falkowski et al., 2004). Such storage capacity permits these diatoms to maintain high division rates for several generations after a pulse of nutrients.

A prerequisite for high growth rates and the ability to form blooms is an efficient and regulated acquisition of inorganic carbon (C_i) that compensates for the catalytic inefficiency of their carbon fixing enzyme ribulose-1,5-bisphosphate carboxylase/oxygenase (RubisCO). This highly conserved enzyme requires CO_2 as substrate, but it has only a poor affinity for this substrate (K_M of 20–70 µmol L^{-1}, Badger et al., 1998). Therefore, at present-day CO_2 concentrations in seawater ranging between 8 and 20 µmol L^{-1} photosynthesis of phytoplankton may suffer from CO_2 limitation. To circumvent this, marine diatoms as well as other phytoplankton taxa operate the so-called carbon concentrating mechanisms (CCMs) that enrich CO_2 at the catalytic site of RubisCO (Giordano et al., 2005; Price et al., 2007; Roberts et al., 2007a). CCMs involve active uptake of CO_2 or HCO_3^- or both. The enzyme carbonic anhydrase (CA), which accelerates the otherwise slow interconversion between HCO_3^- and CO_2, can be located both inside the cell and at the cell surface. Since the loss of the accumulated inorganic carbon (C_i) by CO_2 efflux increases energetic costs and/or decreases the efficiency of a CCM, the ability of a cell to minimize the CO_2 efflux is also an important component of the CCM (Raven and Lucas, 1985; Rost et al., 2006a,b).

Studying the modes of C_i acquisition and assimilation has gained increasing interest given the need to understand the potential effect of rising atmospheric CO_2 levels on overall primary productivity or

* Corresponding author. Alfred Wegener Institute for Polar and Marine Research, Am Handelshafen 12, 27570 Bremerhaven, Germany. Tel.: +49 471 4831 1038; fax: +49 471 4831 2020.
E-mail address: scarlett.trimborn@awi.de (S. Trimborn).

phytoplankton species composition (e.g. Raven and Johnston, 1991; Tortell et al., 2008). The group of diatoms and especially bloom-forming representatives are of particular interest because they strongly influence the vertical fluxes of particular material (Buesseler, 1998). By comparing the apparent half-saturation concentrations ($K_{1/2}$) for photosynthetic CO_2 fixation with the half-saturation constant (K_M) of RubisCO, the presence and the efficiency of a CCM can be assessed (Badger et al., 1998). Relatively efficient CCMs were found in diatoms (Burns and Beardall, 1987; Colman and Rotatore, 1995; Mitchell and Beardall, 1996; Burkhardt et al., 2001; Rost et al., 2003; Trimborn et al., 2008) especially in comparison to other phytoplankton taxa, and these processes are strongly regulated as a function of CO_2 supply (Burkhardt et al., 2001; Rost et al., 2003; Trimborn et al., 2008).

Despite this common feature, diatoms appear to display a high diversity in the way they acquire C_i. It could be shown that diatoms are able to take up both CO_2 and HCO_3^- (Burns and Beardall, 1987; Colman and Rotatore, 1995; Rotatore et al., 1995; Mitchell and Beardall, 1996; Korb et al., 1997; Burkhardt et al., 2001; Rost et al., 2003, 2007; Trimborn et al., 2008), but species differ strongly in the extent to which both carbon sources are utilized (Burkhardt et al., 2001; Rost et al., 2003; Trimborn et al., 2008). Regarding activities of extracellular CA (eCA), diatom species also differed strongly in these studies ranging from activities close to detection limit to some of the highest reported values (Burns and Beardall, 1987; Colman and Rotatore, 1995; Mitchell and Beardall, 1996; Nimer et al., 1997; Burkhardt et al., 2001; Rost et al., 2003; Trimborn et al., 2008). As pointed out by Trimborn et al. (2008), predominant uptake of HCO_3^- or CO_2 generally correlated with high or low eCA activities, respectively. Martin and Tortell (2008) also found this positive correlation between high eCA activities and direct HCO_3^- uptake in 17 diatom species. Opposing the common notion that eCA functions to supply CO_2 to the uptake systems (Elzenga et al., 2000; Sültemeyer, 1998; Colman et al., 2002), Trimborn et al. (2008) suggested that the presence or absence of eCA allows for a more efficient C_i recycling in HCO_3^- and CO_2 users, respectively.

Also controversially discussed in diatoms is the potential role of a C_4-like photosynthetic pathway within carbon assimilation (Reinfelder et al., 2000, 2004; Granum et al., 2005; Roberts et al., 2007a,b; Kroth et al., 2008). This involves the formation of oxaloacetate and malate by phosphoenolpyruvate carboxylase (PEPC), which has the advantage over RubisCO of a high affinity to its carbon source HCO_3^- along with insensitivity to O_2. While evidence for such a pathway comes from experiments with the marine diatom *Thalassiosira weissflogii* (Reinfelder et al., 2000, 2004; Morel et al., 2002), Roberts et al. (2007b) demonstrated that this species relies on an intermediate C_3–C_4 pathway. For *Thalassiosira pseudonana*, RT-PCR as well as ^{14}C short-term labelling experiments could not support C_4-like metabolism (Granum et al., 2005; Roberts et al., 2007b). In contrast, using gene transcript analysis and inhibitor studies McGinn and Morel (2008) concluded that a C_4-like pathway would operate in *T. pseudonana* and *Phaeodactylum tricornutum*. The possibility of a C_4-like pathway in other diatom species has not yet been investigated.

The aim of this study was to improve our understanding of the modes of carbon acquisition and to clarify whether a C_4-like pathway may operate in four diatom species. As bloom-forming representatives we chose *Eucampia zodiacus* (Hobson and McQuoid, 1997), *Skeletonema costatum* (Marshall, 1976; Hobson and McQuoid, 1997) and *Thalassionema nitzschioides* (Marshall, 1976, 1978; Edwards et al., 2005) and as non-bloom-forming species the coastal marine diatom *T. pseudonana* for which the genome has been recently sequenced (Armbrust et al., 2004). Photosynthetic O_2 evolution as well as CO_2 and HCO_3^- uptake were quantified during steady-state photosynthesis by means of a membrane-inlet mass spectrometry (MIMS). To characterise the CCM of each species further, measurements of intracellular and extracellular CA activities were performed by monitoring ^{18}O exchange from doubly labelled $^{13}C^{18}O_2$. RubisCO

and PEPC activities were measured to provide insights into the biochemical mechanisms of intracellular C assimilation.

2. Material and methods

2.1. Culture and experimental conditions

T. nitzschioides and *E. zodiacus* (both species isolated from the North Sea by Anne Schwaderer in 2004), *S. costatum* (CCMP 1332) and *T. pseudonana* (CCMP 1335) were grown at 15 °C in semi-continuous dilute batch cultures using sterile-filtered (0.2 µm) unbuffered seawater, enriched with nutrients, silicate, trace metals and vitamins according to F/2 medium (Guillard and Ryther, 1962). Experiments were carried out using a light:dark cycle of 16:8 h at an incident light intensity of 200 µmol photons m^{-2} s^{-1}. Cultures as well as the respective dilution media were continuously sparged with air containing CO_2 partial pressures (pCO$_2$) of 50, 370, 800 µatm resulting in pH values of 8.9, 8.2, and 7.9, respectively, on the National Bureau of Standards (NBS) scale. CO_2 gas mixtures were generated with gas-mixing pumps (Woesthoff GmbH, Bochum, Germany), using CO_2-free air (Nitrox CO$_2$ RP280, Domnick Hunter ltd., Willich, Germany), pure CO_2 (Air Liquide Deutschland ltd., Germany), or ambient air, respectively. pH was measured using a pH-meter (WTW, model pMX 3000/pH, Weilheim, Germany) that was calibrated (2-point calibration) on a daily basis. Daily dilutions with the corresponding acclimation media ensured that the pH level remained constant and that the cells stayed in the mid-exponential growth phase. Cultures in which the pH had shifted significantly (>0.05 U) in comparison to cell-free medium at the respective pCO$_2$ were excluded from further analysis.

2.2. Determination of seawater carbonate chemistry

Alkalinity samples were taken from the filtrate (Whatman GFF filter, ~0.6 µm), stored in 300-mL borosilicate flasks at 4 °C and measured by potentiometric titration with an average precision of 8 µmol kg^{-1} (Brewer et al., 1986). Total alkalinity was calculated from linear Gran Plots (Gran, 1952). The carbonate system was calculated from alkalinity, pH, silicate, phosphate, temperature, and salinity using the CO2Sys program (Lewis and Wallace, 1998). Equilibrium constants of Mehrbach et al. (1973) refitted by Dickson and Millero (1987) were chosen. The parameters of the carbonate system for the respective treatments are given in Table 1.

2.3. Sampling

After acclimation to 370 and 800 µatm for at least 3 days, cells were harvested by gentle filtration over a 3 µm membrane filter (Isopore, Millipore) 4 to 8 h after the beginning of the photoperiod to allow photosynthesis and CCM activity to be fully induced. Subsequently, the cells were washed with CO_2-free F/2 medium buffered with 50 mmol L^{-1} 2-[4-(2-Hydroxyethyl)-1-piperazinyl]ethanesulfonic acid (HEPES, pH 8.0). The samples were then used for measuring inorganic carbon (C_i) fluxes and CA activities with the MIMS. Samples for determination of chlorophyll *a* (Chl *a*) concentration were taken after the measurements and stored at −80 °C. Chl *a* was subsequently

Table 1
Parameters of the seawater carbonate system were calculated from alkalinity, pH, silicate, phosphate, temperature, and salinity using the CO2Sys program (Lewis and Wallace, 1998).

	pCO$_2$ (µatm)	CO$_2$ (µmol kg^{-1})	DIC (µmol kg^{-1})	TA (µEq kg^{-1})	pH (NBS)
High pCO$_2$	803 ± 8	31 ± 0.3	2176 ± 21	2309 ± 21	7.90 ± 0.03
Ambient pCO$_2$	369 ± 3	14 ± 0.1	2059 ± 19	2317 ± 15	8.20 ± 0.03
Low pCO$_2$	51 ± 0.2	1.9 ± 0.03	1567 ± 40	2297 ± 9	8.85 ± 0.03

Values represent the means of at least twelve replicate incubations (± SD).

extracted in 10 mL acetone (overnight in darkness, at 4 °C) and determined with a Turner Designs Fluorometer (Model 10-000 R, Mt. View, Canada).

2.4. Determination of CA activity

Activity of extracellular and intracellular CA was determined by measuring the loss of ^{18}O from doubly labelled $^{13}C^{18}O_2$ to water caused by the interconversion of CO_2 and HCO_3^- (Silverman, 1982). The determination of CA activity was performed with a sector field multicollector mass spectrometer (Isoprime, GV Instruments, Manchester, UK) via a gas-permeable polytetrafluoroethylene membrane (PTFE, 0.01 mm) inlet system. The reaction sequence of ^{18}O loss from initial $^{13}C^{18}O^{18}O$ ($m/z = 49$), via the intermediate $^{13}C^{18}O^{16}O$ ($m/z = 47$) to the final molecule $^{13}C^{16}O^{16}O$ ($m/z = 45$) was recorded continuously. The ^{18}O enrichment was calculated as:

$$^{18}O \ \log(\text{enrichment}) = \log \frac{(^{13}C^{18}O_2) \times 100}{^{13}CO_2} \tag{1}$$

$$= \log \frac{(m/z\,49) \times 100}{m/z\,45 + m/z\,47 + m/z\,49}$$

CA measurements were performed in 8 mL of F/2 medium buffered with 50 mmol L^{-1} HEPES (pH 8.0) at 15 °C. To avoid interference with light-dependent C_i uptake by the cells, all measurements were carried out in the dark (Palmqvist et al., 1994). After adding $NaH^{13}C^{18}O_3$ to a final concentration of 1 mmol L^{-1} and chemical equilibration, the uncatalyzed ^{18}O loss was monitored for about 8 min prior to the addition of cells. Extracellular CA activity (eCA) was calculated from the increasing rate of ^{18}O depletion after the addition of the cells (slope S_2) in comparison to the uncatalyzed reaction (slope S_1) and normalized on a Chl a basis (Badger and Price, 1989):

$$U = \frac{(S_2 - S_1) \times 100}{S_1 \times \mu g\, \text{Chl}\, a} \tag{2}$$

Intracellular CA activity was determined in the presence of 100 μmol L^{-1} dextran-bound sulfonamide (DBS), an inhibitor of eCA. The drop in the log(enrichment) was calculated by extrapolation of S_2 back to the time of cell injection (Δ as defined by Palmqvist et al., 1994). Values of Δ are expressed in arbitrary units per μg Chl a. Chl a concentrations in CA assays ranged from 0.11 to 1.16 μg mL^{-1}.

2.5. Determination of net photosynthesis, CO_2 and HCO_3^- uptake

The C_i fluxes were determined during steady-state photosynthesis with the same membrane-inlet mass spectrometer as for the CA measurements. The method established by Badger et al. (1994) uses the chemical disequilibrium between CO_2 and HCO_3^- fluxes during light-dependent C_i uptake to differentiate between CO_2 and HCO_3^- fluxes across the plasmalemma. C_i flux estimates are based on simultaneous measurements of O_2 and CO_2 during consecutive light and dark intervals. During dark intervals, known amounts of C_i are added to measure rates as a function of CO_2 and HCO_3^- concentrations. Rates of O_2 consumption in the dark and O_2 evolution in the light provide a direct estimate of respiration and net C_i fixation under the assumption of a respiratory quotient of 1 and a photosynthetic quotient of 1.1 to convert O_2 fluxes into C_i fluxes (e.g. Asmus, 1982; Mills and Wilkinson, 1986; Badger et al., 1994; Wolfstein and Hartig, 1998; Rost et al., 2007). Net CO_2 uptake is calculated from the steady-state rate of CO_2 depletion at the end of the light period, corrected for the CO_2/HCO_3^- interconversion in the medium. The HCO_3^- uptake is derived by a mass balance equation, i.e. the difference between net C_i fixation and net CO_2 uptake. All measurements were performed in initially CO_2-free F/2 medium buffered with 50 mmol L^{-1} HEPES (pH 8.0) at 15 °C. The presence of

DBS (100 μmol L^{-1}) ensured the complete inhibition of any eCA activity in all tested species (data not shown). Light and dark intervals during the assay lasted for 6 min. The incident photon flux density was 300 μmol photons $m^{-2} s^{-1}$. Further details on the method and calculations are given in Badger et al. (1994) and Rost et al. (2007). Chl a concentrations in the assay ranged from 0.54 to 1.58 μg mL^{-1}.

2.6. Carbon isotope fractionation

Samples for particulate organic carbon (POC) were filtered onto precombusted (500 °C, 12 h) GFF filters (~0.6 μm) and stored in precombusted (500 °C, 12 h) Petri dishes at −20 °C. Prior to analysis, POC filters were fumed with HCl for 2 h to remove all inorganic carbon. POC and related $\delta^{13}C$ values were subsequently measured in duplicate on an EA mass spectrometer (ANCA-SL 2020, Sercon Ltd., Crewe, UK), with a precision of ±0.5‰, respectively. The isotopic composition is reported relative to the PeeDee belemnite standard (PDB):

$$\delta^{13}C_{\text{Sample}} = \left[\frac{(^{13}C /^{12}C)_{\text{Sample}}}{(^{13}C /^{12}C)_{\text{PDB}}} - 1 \right] \times 1000 \tag{3}$$

Isotope fractionation during POC formation (ε_p) was calculated relative to the isotopic composition of CO_2 in the medium (Freeman and Hayes, 1992):

$$\varepsilon_p = \frac{\delta^{13}C_{CO_2} - \delta^{13}C_{POC}}{1 + \frac{\delta^{13}C_{POC}}{1000}} \tag{4}$$

To determine isotopic composition of DIC ($\delta^{13}C_{DIC}$), samples were sterile-filtered (0.2 μm), fixed with $HgCl_2$ (~140 mg L^{-1} final concentration), and stored at 4 °C. Measurements of $\delta^{13}C_{DIC}$ were performed with a Finnegan mass spectrometer (MAT 252) at a precision of $\delta^{13}C = \pm 0.05$‰. The isotopic composition of CO_2 ($\delta^{13}C_{CO2}$) was calculated from $\delta^{13}C_{DIC}$, making use of a mass balance relation (see Zeebe and Wolf-Gladrow, 2001):

$$\delta^{13}C_{HCO_3^-} = \frac{\delta^{13}C_{DIC}\,[DIC] - (\varepsilon_a[CO_2] + \varepsilon_b[CO_3^{2-}])}{(1 + \varepsilon_a \times 10^{-3})[CO_2] + [HCO_3^-] + (1 + \varepsilon_b \times 10^{-3})[CO_3^{2-}]} \tag{5}$$

$$\delta^{13}C_{CO_2} = \delta^{13}C_{HCO_3^-}(1 + \varepsilon_a \times 10^{-3}) + \varepsilon_a \tag{6}$$

Temperature-dependent fractionation factors between CO_2 and HCO_3^- (ε_a) as well as HCO_3^- and CO_3^{2-} (ε_b) are given by Mook (1986) and Zhang et al. (1995), respectively.

2.7. Determination of RubisCO and PEPC activities

The activities of RubisCO and PEPC were determined using ^{14}C-based assays modified from Descolas-Gros and Oriol (1992), MacIntyre et al. (1997), Reinfelder et al. (2000), and Tortell et al. (2006). The assays measure the rate of ^{14}C incorporation into organic (acid stable) carbon products following the addition of $H^{14}CO_3^-/^{14}CO_2$ and ribulose bisphosphate (RuBP) or phosphoenolpyruvate (PEP). In the present study, we largely followed the protocol described by Tortell et al. (2006) with a few modifications.

Cells acclimated to 50, 370, and 800 μatm were concentrated by filtration over a 3 μm membrane filter (Isopore, Millipore). Subsequently, 15 mL of the concentrated cell suspension was transferred to a falcon tube and placed on ice. The samples were then concentrated by centrifugation at 4000 rpm (centrifuge Jouan, Model BR4i, Saint Herblain, France) for 10 min at 0 °C. The pellet was resuspended with 2 mL ice-cold extraction/assay buffer and transferred into a 2 mL Apex vial. The buffer, modified
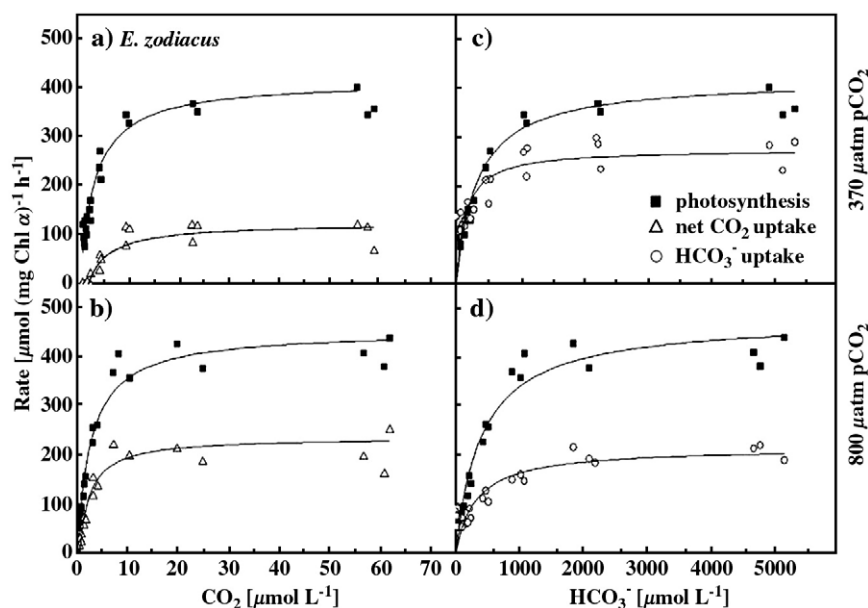
Fig. 1. *E. zodiacus*. Rates of net photosynthesis, net CO_2 uptake and HCO_3^- uptake as a function of CO_2 and HCO_3^- concentration in the assay medium. The cultures were acclimated to 370 µatm (a, b) and 800 µatm (c, d) of CO_2 for at least 3 d. Michaelis–Menten fits were obtained from at least three individual measurements.

from MacIntyre et al. (1997) contained 50 mmol L^{-1} N,N-Bis(2-hydroxyethyl) glycine (BICINE, pH 7.5), 1 mmol L^{-1} ethylenediaminetetraacetic acid (EDTA), 10 mmol L^{-1} MgCl$_2$, 1.5 mol L^{-1} glycerol, 10 mmol L^{-1} NaHCO$_3$, 5 mg L^{-1} bovine serum albumin, 0.2% Triton-X, and 5 mmol L^{-1} dithiotrietol (DTT). The samples were then homogenized in a glass grinding tube, which was placed in an ice-containing tumbler, with a rotating glass pestle (EUROSTAR digital, IKA-Werke, Staufen, Germany) at 1000 rpm for 3 intervals of 30 s. Subsequently, samples were sonicated (Branson Sonifier 450, Schwäbisch Gmünd, Germany) with a microtip at 70% duty cycle for 3 intervals of 30 s at −2 °C. Crude cell extracts were then clarified by centrifugation (Centrifuge Hettich, Mikro 22R, Schnakenberg, Germany) at 14,000 rpm for 30 s at 0 °C, and the supernatants retained for enzyme assays.

After extraction, seven 200 µL aliquots were taken from the supernatant and dispensed into a microtip, two replicates each for blank, RubisCO and PEPC activity. Then, samples were preincubated over 15 min in the dark leading to the depletion of residual RuBP and PEP in the homogenates. With the exception of the blank, 20 µL of either the RuBP stock (23 mmol L^{-1}) or the PEP stock (50 mmol L^{-1}) was added to the subsamples. Stock solutions of RuBP and PEP were both stored frozen at −20 °C. After a 3-min incubation at 20 °C in the light (e.g. MacIntyre and Geider, 1996; MacIntyre et al., 1997), a 5 µCi spike of NaH^{14}CO$_3^-$ (CFA3, GE Healthcare, Freiburg, Germany) was injected into all samples to initiate ^{14}C fixation. After 30 min, reactions were terminated by the addition of 100 µL HCl (6 mol L^{-1}). To remove residual inorganic ^{14}C that had not been fixed, samples were placed in a fume hood on a shaker table and left to degas for at least 24 h. Degassed samples were then transferred into 7-mL scintillation vials and 5 mL of scintillation cocktail (Ultima Gold AB, Perkin Elmer, Boston, MA, USA) was added. Afterwards, ^{14}C was measured by means of the scintillation counter TriCarb 2100 TR
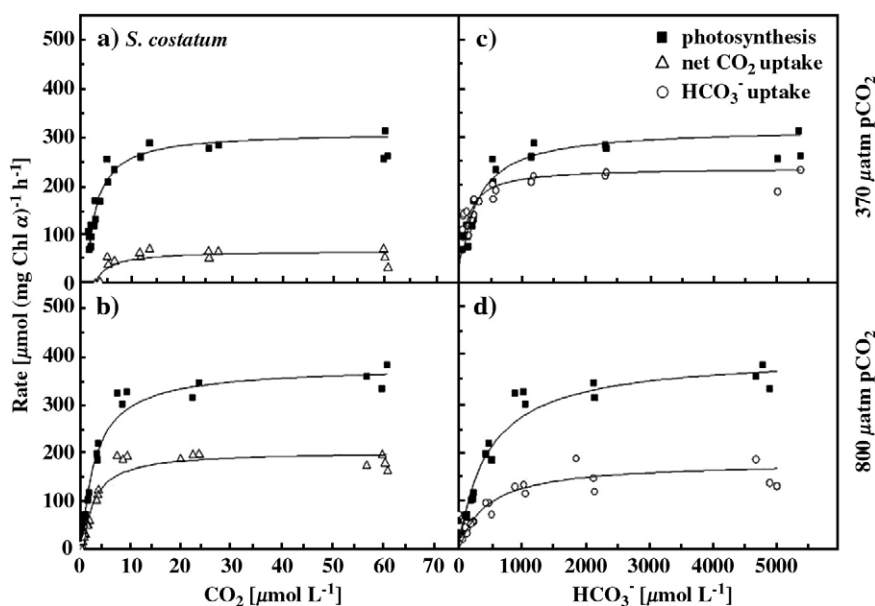

Fig. 2. *S. costatum*. Rates of net photosynthesis, net CO_2 uptake and HCO_3^- uptake as a function of CO_2 and HCO_3^- concentration in the assay medium. The cultures were acclimated to 370 µatm (a, b) and 800 µatm (c, d) of CO_2 for at least 3 d. Michaelis–Menten fits were obtained from at least three individual measurements.

Fig. 3. T. nitzschioides. Rates of net photosynthesis, net CO_2 uptake and HCO_3^- uptake as a function of CO_2 and HCO_3^- concentration in the assay medium. The cultures were acclimated to 370 μatm (a, b) and 800 μatm (c, d) of CO_2 for at least 3 d. Michaelis–Menten fits were obtained from at least three individual measurements.
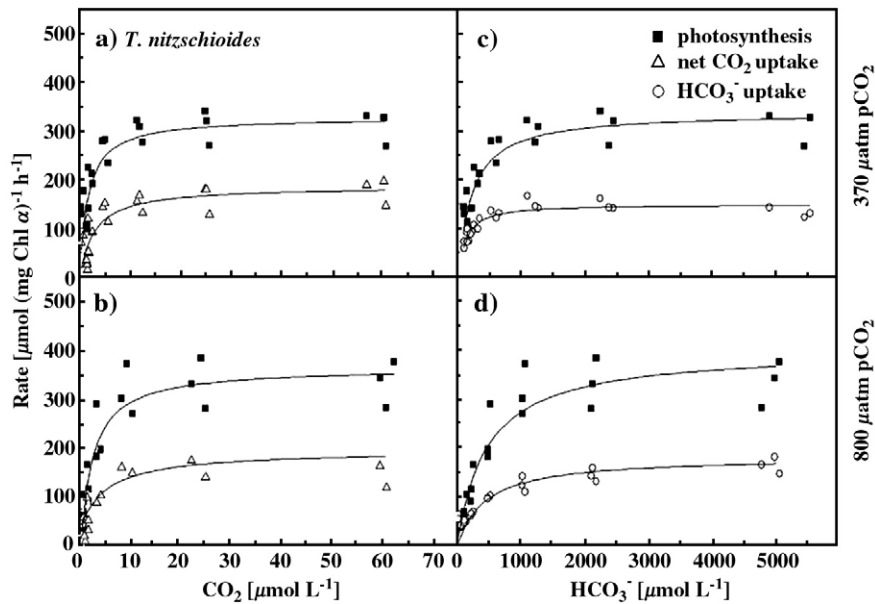
(Canberra, Australia). Radioactivity in the blanks (^{14}C added without substrates) was subtracted from all samples.

3. Results

3.1. Photosynthesis and C_i fluxes

Net photosynthesis, net CO_2 uptake and HCO_3^- uptake are shown as a function of CO_2 and/or HCO_3^- concentration for E. zodiacus, S. costatum, T. nitzschioides, and T. pseudonana (Figs. 1–4) acclimated to ambient (370 μatm) and high (800 μatm) pCO$_2$ levels. Simultaneous uptake of CO_2 and HCO_3^- during steady-state photosynthesis was observed in all investigated species. The corresponding kinetic parameters such as half-

saturation concentrations ($K_{1/2}$) and maximum rates (V_{max}) were obtained from a Michaelis–Menten fit and are summarized in Table 2.

With values between 1.9 and 4.0 μmol CO_2 L^{-1} for all investigated diatom species, the $K_{1/2}$ (CO_2) values for photosynthesis were about one order of magnitude lower than the K_M (CO_2) values known for RubisCO in marine diatoms (~31–41 μmol CO_2 L^{-1}, Badger et al., 1998). The $K_{1/2}$ values for photosynthesis decreased from 443 μmol to 265 μmol DIC L^{-1} in S. costatum and from 380 μmol to 223 μmol DIC L^{-1} in T. nitzschioides with decreasing pCO$_2$ in the acclimation (t-test, *p<0.05), in comparison the $K_{1/2}$ values were similar in E. zodiacus and T. pseudonana at both pCO$_2$ levels (t-test, p>0.05; Figs. 1–4, Table 2). The V_{max} of photosynthesis remained constant in E. zodiacus, T. nitzschioides and T. pseudonana (t-test, p>0.05) while V_{max} increased with increasing pCO$_2$ in S. costatum (t-test, *p<0.05; Figs. 1–4, Table 2).
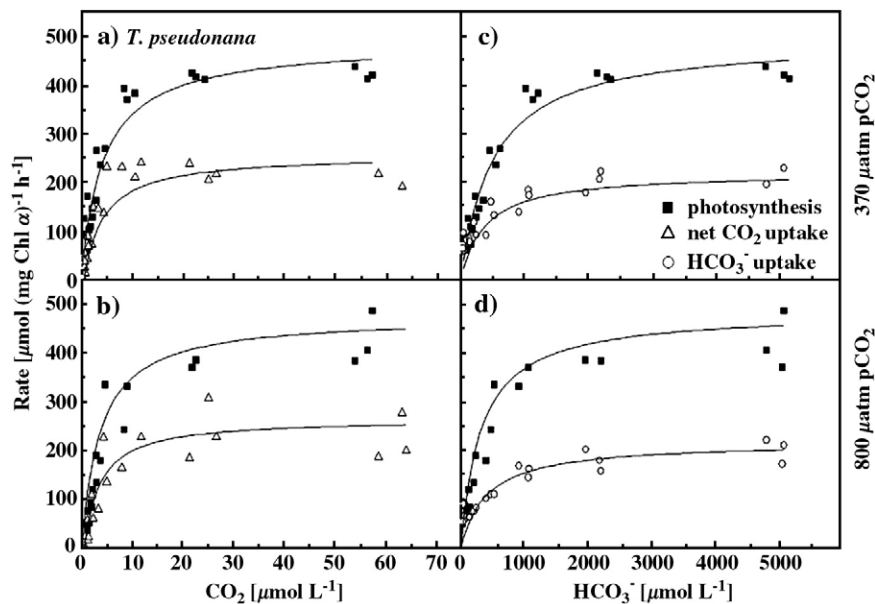

Fig. 4. T. pseudonana. Rates of net photosynthesis, net CO_2 uptake and HCO_3^- uptake as a function of CO_2 and HCO_3^- concentration in the assay medium. The cultures were acclimated to 370 μatm (a, b) and 800 μatm (c, d) of CO_2 for at least 3 d. Michaelis–Menten fits were obtained from at least three individual measurements.

Table 2
$K_{1/2}$ and V_{max} values for photosynthesis, net CO_2 uptake, and HCO_3^- uptake for *E. zodiacus*, *S. costatum*, *T. nitzschioides* and *T. pseudonana* acclimated to ambient and high CO_2 concentrations.

pCO$_2$	Photosynthesis			Net CO$_2$ uptake		HCO$_3^-$ uptake	
(µatm)	$K_{1/2}$ (CO$_2$)	$K_{1/2}$ (DIC)	V_{max}	$K_{1/2}$ (CO$_2$)	V_{max}	$K_{1/2}$ (HCO$_3^-$)	V_{max}
E. zodiacus							
370	2.9 ± 0.4	323 ± 53	414 ± 19	2.6 ± 0.5	123 ± 7	140 ± 40	274 ± 19
800	3.6 ± 0.5	411 ± 63	454 ± 16	6.6 ± 1.4	234 ± 3	325 ± 101	214 ± 19
S. costatum							
370	2.8 ± 0.4	265 ± 53	309 ± 14	2.8 ± 0.4	65 ± 6	113 ± 22	236 ± 10
800	3.1 ± 0.4	441 ± 74	371 ± 14	6.0 ± 0.9	208 ± 3	383 ± 94	168 ± 12
T. nitzschioides							
370	1.9 ± 0.6	223 ± 41	342 ± 23	2.7 ± 1.0	195 ± 4	130 ± 15	149 ± 6
800	2.7 ± 0.6	379 ± 78	364 ± 23	3.6 ± 1.6	200 ± 3	294 ± 77	164 ± 12
T. pseudonana							
370	3.4 ± 0.8	513 ± 86	484 ± 30	3.8 ± 1.2	253 ± 4	463 ± 73	228 ± 11
800	4.0 ± 0.9	443 ± 98	470 ± 28	3.4 ± 1.1	262 ± 4	380 ± 96	212 ± 15

Kinetic parameters were calculated from a Michaelis–Menten fit to the combined data. Values for $K_{1/2}$ and V_{max} are given in µmol L^{-1} and µmol (mg Chl a)$^{-1}$ h^{-1}, respectively. Values represent the means of triplicate incubations ($\pm$SD).

The $K_{1/2}$ and V_{max} for net CO_2 uptake remained constant in *T. nitzschioides* and *T. pseudonana* independent of the pCO$_2$ level (*t*-test, $p > 0.05$) while both parameters increased with increasing pCO$_2$ in *E. zodiacus* and *S. costatum* (*t*-test, ***$p < 0.001$; Figs. 1–4, Table 2). Among the investigated species, *T. pseudonana* displayed the highest V_{max} for net CO_2 uptake. $K_{1/2}$ values for HCO_3^- uptake strongly decreased in all investigated species with decreasing pCO$_2$ (*t*-test, *$p < 0.05$) with the exception of *T. pseudonana*, for which the affinities remained unaffected over the tested range of pCO$_2$ (*t*-test, $p > 0.05$). In *E. zodiacus* and *S. costatum*, V_{max} of HCO_3^- uptake increased with increasing pCO$_2$ level (*t*-test, *$p < 0.05$), while V_{max} remained constant in *T. nitzschioides* and *T. pseudonana* (*t*-test, $p > 0.05$).

Using the uptake kinetics obtained in the assay, the contribution of HCO_3^- uptake relative to carbon fixation was estimated (Fig. 5). At the ambient pCO$_2$ level, *E. zodiacus* and *S. costatum* obtained the highest relative HCO_3^- contribution with ~80% while at elevated pCO$_2$ both carbon sources contributed equally to net fixation. For *T. nitzschioides* and *T. pseudonana*, the contribution of HCO_3^- to net fixation was ~50% independent of the pCO$_2$ in the acclimation.
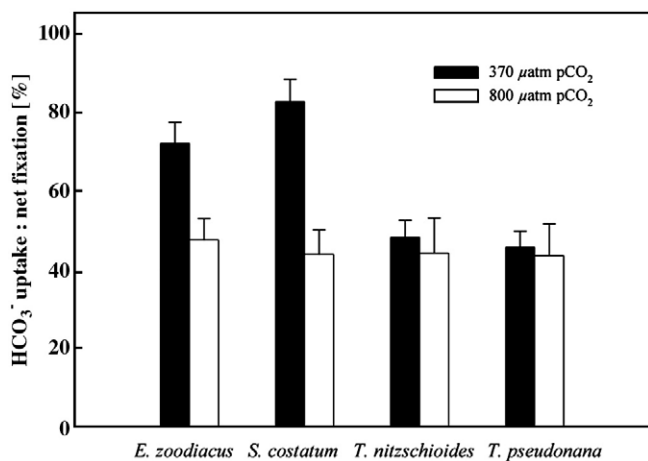

Fig. 6. Activities of eCA (a) and iCA (b) activities from cells acclimated to 370 µatm and 800 µatm CO_2. Values represent the means of triplicate incubations ($\pm$SD).

3.2. Extra- and intracellular CA activity

With the exception of *T. pseudonana*, for which eCA activities were constant in all acclimations (*t*-test, $p > 0.05$; Fig. 6a), eCA activities strongly increased with decreasing pCO$_2$ in the other investigated species (*t*-test, ***$p < 0.001$). In comparison, the highest eCA activities were exhibited by *E. zodiacus* with values of ~940 U (µg Chl a)$^{-1}$ at ambient CO_2 concentrations and lowest by *T. pseudonana* with values

Fig. 5. Ratios of HCO_3^- uptake:net photosynthesis of cells acclimated to 370 µatm and 800 µatm CO_2. Ratios were based on the rates obtained at Ci concentrations of about 2 mmol L^{-1} in at least three individual MIMS measurements.
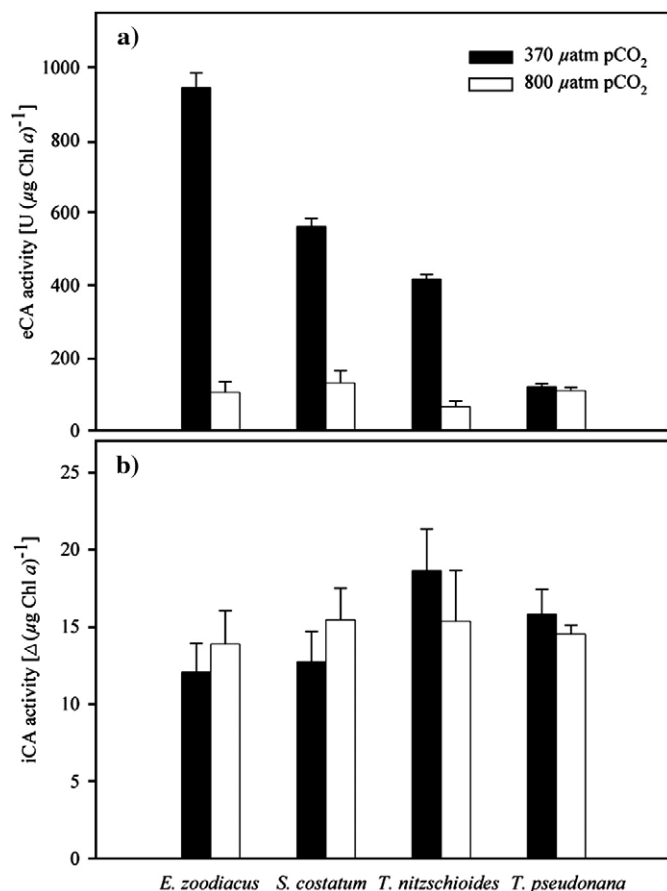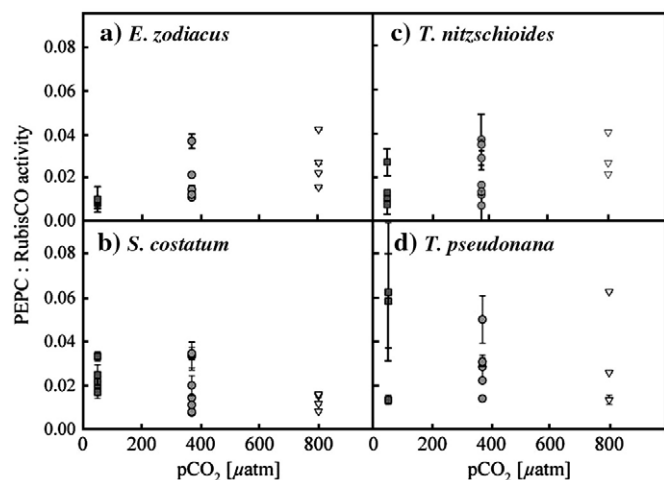

Fig. 7. The relative ratios of PEPC activity:RubisCO activity of cells acclimated to 50, 370, and 800 µatm CO_2. Error bars denote $\pm$SD ($n \geq 3$).
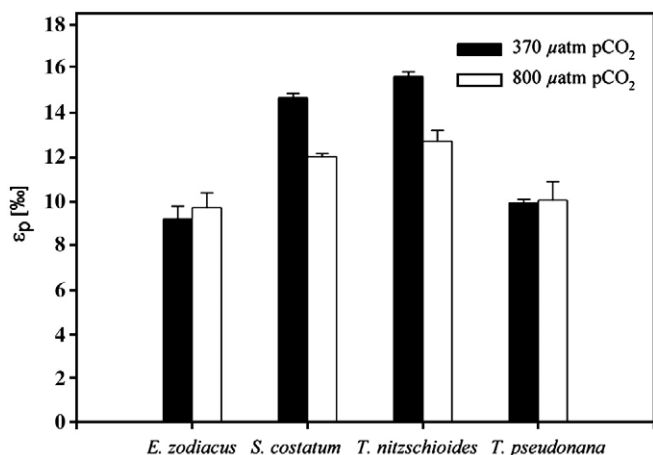
Fig. 8. Isotope fractionation (ε_p) from cells acclimated to 370 μatm and 800 μatm CO_2. Values for ε_p have been calculated from the $^{13}C_{CO_2}$ and $^{13}C_{POC}$ in the respective acclimations of each species. Error bars denote ± SD ($n = 3$).

of ~120 U (μg Chl a)$^{-1}$. Intracellular CA activities were largely unaffected by the pCO_2 in the acclimation (t-test, $p > 0.05$; Fig. 6b). In all investigated species, values for internal CA activities were similar.

3.3. Activities of PEPC and RubisCO

The activities of PEPC averaged generally less than 3% of those observed for RubisCO. While the PEPC/RubisCO ratio decreased in *E. zodiacus* and *T. nitzschioides* with decreasing pCO_2 in the acclimation (ANOVA, F-test, ***$p < 0.001$; Fig. 7a, c), for *S. costatum* variations in the ratio were significant between the 800 μatm and the 370 μatm pCO_2 treatments (ANOVA, Bonferroni's multiple comparison test, ***$p < 0.001$), but not from 370 μatm down to 50 μatm pCO_2 (ANOVA, Bonferroni's multiple comparison test, $p > 0.05$; Fig. 7b). For *T. pseudonana*, the ratio remained constant independent of the pCO_2 (ANOVA, F-test, $p > 0.05$; Fig. 7d).

3.4. Carbon isotope fractionation

With the exception of *T. nitzschioides* and *S. costatum* (t-test, ***$p < 0.001$), carbon isotope fractionation was not affected by pCO_2 (t-test, $p > 0.05$; Fig. 8). While *S. costatum* and *T. nitzschioides* obtained the highest fractionation with values up to 15.6‰, for *E. zodiacus* and *T. pseudonana* ε_p values were ~9.5‰.

4. Discussion

In the present study, we investigated carbon acquisition and intracellular assimilation in three bloom-forming diatoms and *T. pseudonana* in response to changes in CO_2 supply. By means of MIMS techniques in combination with ^{14}C-based assays and analysis of ^{13}C fractionation, different components of the CCM were characterised in each species. C_i uptake kinetics and extracellular CA activities were highly regulated in the investigated bloom-forming species while *T. pseudonana* displayed a very efficient, but not regulated CCM in response to the tested CO_2 range (Table 2, Figs. 1–4, 6a).

4.1. Photosynthetic O_2 evolution

By comparing the $K_{1/2}$ (CO_2) for photosynthesis with the K_M of the few investigated RubisCOs of diatoms (~31–41 μmol CO_2 L^{-1}), the presence and the efficiency of a CCM can be assessed (Badger et al., 1998). In this case, the term 'efficiency' relates to the ability of a cell to reach C_i-saturation in relation to DIC availability. The $K_{1/2}$ (CO_2) values for photosynthesis ranged between 1.9 and 4.0 μmol CO_2 L^{-1} in

the investigated species (Table 2, Figs. 1–4) indicating the operation of highly efficient CCMs. As for other marine diatom species, our findings are consistent with previously published $K_{1/2}$ values for photosynthesis obtained by MIMS (Burkhardt et al., 2001; Rost et al., 2003; Trimborn et al., 2008) or by measurements of photosynthetic O_2 evolution in response to varying C_i concentrations (Burns and Beardall, 1987; Colman and Rotatore, 1995).

Another indication for the operation of a CCM are changes in affinities as a function of the acclimation conditions. This up- and down-regulation in $K_{1/2}$ values for photosynthesis in response to CO_2 supply has been observed in the two bloom-forming species *S. costatum* and *T. nitzschioides*, but not in *E. zodiacus* and *T. pseudonana* at the investigated pCO_2 levels. In agreement to our study, Rost et al. (2003) demonstrated for a strain of *S. costatum* (an isolate from the North Sea) that $K_{1/2}$ values for photosynthesis were ~250 μmol DIC L^{-1} and 500 μmol DIC L^{-1} in cells acclimated to ambient and 1800 μatm pCO_2, respectively. Using the same strain of *T. pseudonana* as in our study, Fielding et al. (1998) performed measurements of photosynthetic O_2 evolution in cells acclimated to DIC concentrations ranging from 0.2 to 2.75 mmol L^{-1}. From their results, low CCM regulation in *T. pseudonana* under ambient and high pCO_2 can be deduced as $K_{1/2}$ values for photosynthetic O_2 evolution were similar with ~460 and ~480 μmol DIC L^{-1} under the respective DIC concentrations of 2.06 mmol and 2.18 mmol DIC L^{-1} (see Table 1).

Overall, the generally low $K_{1/2}$ values for photosynthesis suggest that all investigated species possess highly efficient CCMs at the investigated pCO_2 levels. With respect to the ability of a species to regulate its CCM in response to CO_2, the acclimation of cells to ambient and high pCO_2 levels revealed that the two bloom-forming species *S. costatum* and *T. nitzschioides* operate strongly regulated CCMs in contrast to *T. pseudonana* and *E. zodiacus*. However, to gain more information about the underlying mechanisms that determine the efficiency and the regulation of a CCM, the individual components of the CCM such as the carbon sources and their uptake kinetics, the extra- and intracellular CA activities as well as the intracellular assimilation pathway will be discussed in the following paragraphs.

4.2. Carbon sources and uptake kinetics

In agreement with previous studies on carbon acquisition in marine diatoms (e.g., Burns and Beardall, 1987; Colman and Rotatore, 1995; Rotatore et al., 1995; Korb et al., 1997), simultaneous uptake of CO_2 and HCO_3^- was observed in the investigated diatom species (Table 2, Figs. 1–4). In addition to the estimates of the C_i sources, HCO_3^- and CO_2 uptake kinetics were determined during steady-state photosynthesis using the equations of Badger et al. (1994). According to our results, the preference for carbon species and C_i uptake kinetics differed among the investigated diatom species.

The two bloom-forming species *E. zodiacus* and *S. costatum* were characterised by a strong preference for HCO_3^- at ambient pCO_2 while both species used CO_2 and HCO_3^- in equal quantities at high pCO_2 (Fig. 5). Korb et al. (1997) demonstrated by means of ^{14}C-disequilibrium technique that *S. costatum* was able to take up HCO_3^-, but did not quantify the rate or its contribution to photosynthesis. As in the present study, Rost et al. (2003) obtained an increasing preference for HCO_3^- with decreasing CO_2 concentrations in another strain of *S. costatum*. Such an up-regulation in HCO_3^- transport, as was observed for the two bloom-forming species *E. zodiacus* and *S. costatum* (Table 2), might be ascribed to both an increasing number of HCO_3^- transporters and the induction of high affinity HCO_3^- uptake systems under these conditions. In contrast to the species above, *T. nitzschioides* and *T. pseudonana* did not alter the relative contributions of HCO_3^- or CO_2 as a function of CO_2 supply (Fig. 5). While the bloom-forming *T. nitzschioides* compensated for decreasing CO_2 supply during acclimation by strongly increasing substrate affinities of the HCO_3^- uptake system, C_i uptake kinetics of the non-bloom-forming *T. pseudonana* hardly responded to the tested pCO_2 levels (Table 2). For *T. nitzschioides*, the increase in substrate affinity could be either due to

posttranslational modifications (Sültemeyer et al., 1998) or to an increasing expression of a high affinity uptake system (e.g. Shibata et al., 2002). According to Elzenga et al. (2000), who applied the ^{14}C-disequilibrium technique, *T. pseudonana* solely relied on HCO_3^-, which stands in contrast to our results. Despite differences in the approach taken between Elzenga et al. (2000) and the present study, a recent method comparison showed that MIMS and ^{14}C-disequilibrium technique yield identical estimates for the HCO_3^- contribution to net carbon fixation (Rost et al., 2007). The higher HCO_3^- contribution for *T. pseudonana* obtained by Elzenga et al. (2000) may have been the result of the rather high rate constants (α_1 and α_2) as well as the low CO_2 equilibrium concentration for the pH 7.0 spike used in their fit function.

According to our results, bloom-forming diatom species possess highly regulated C_i uptake systems when exposed to ambient and high pCO_2 levels while C_i uptake kinetics hardly responded in the non-bloom-forming *T. pseudonana* under these conditions. A high plasticity in the preference for CO_2 or HCO_3^- as well as the ability to regulate the affinities of C_i uptake systems has been reported previously for the group of diatoms, in particular for bloom-forming representatives (e.g. Burkhardt et al., 2001; Trimborn et al., 2008). Such high flexibility in the use of C_i sources appears to be exceptional, especially when compared to other taxa like dinoflagellates or cyanobacteria (Nimer et al., 1999; Leggat et al., 1999; Dason et al., 2004; Rost et al., 2006a; Price et al., 2007; Ratti et al., 2007).

4.3. Carbonic anhydrase activity

The enzyme carbonic anhydrase is considered to be an important component of the CCM (Sültemeyer, 1998; Badger, 2003; Moroney and Ynalvez, 2007) as it catalyses the conversion between HCO_3^- and CO_2. In agreement with previous investigations (Nimer et al., 1997; Burkhardt et al., 2001; Rost et al., 2003; Trimborn et al., 2008), externally located CA was found to be up-regulated with decreasing CO_2 supply in all tested diatom species except for *T. pseudonana* (Fig. 6a). Highest eCA activities were found in the bloom-forming species with values up to 940 U (µg Chl $a)^{-1}$ for *E. zodiacus* while *T. pseudonana* displayed lowest eCA activities of 120 U (µg Chl $a)^{-1}$. These values correspond to an enhancement of the spontaneous HCO_3^-/CO_2 interconversion by 940% and 120% per µg Chl a. For *T. pseudonana*, the absence of significant eCA activities has also been verified using either the ^{14}C-disequilibrium technique (Elzenga et al., 2000) or the potentiometric method (Nimer et al., 1997). Therefore, we conclude that eCA plays an important role in the carbon acquisition of bloom-forming diatom species while eCA activities are negligible in *T. pseudonana*.

It has been a common notion that eCA functions to increase the CO_2 concentration in the boundary layer by converting HCO_3^- to CO_2 and herewith facilitate CO_2 uptake (e.g. Badger and Price, 1994; Sültemeyer, 1998; Elzenga et al., 2000; Tortell et al., 2006). However, results from model calculations indicated that eCA activities may be insufficient to significantly enhance CO_2 supply in marine microalgae with a cell radius of 10 µm or less (Wolf-Gladrow and Riebesell, 1997). Furthermore, high eCA activities are often induced under elevated pH, hence low CO_2 equilibrium concentrations, and correlate with predominant uptake of HCO_3^- (Burkhardt et al., 2001; Rost et al., 2003; Trimborn et al., 2008; Martin and Tortell, 2008). Based on these observations from laboratory and field experiments, Trimborn et al. (2008) proposed that eCA acts to convert effluxing CO_2 to HCO_3^-, which is subsequently taken up via the HCO_3^- transporter. Such a C_i recycling mechanism would be most efficient when CA-mediated conversion is localized to the periplasmic space, i.e. in close vicinity of the HCO_3^- transporter. The results of the present study, i.e. high eCA activities in concert with a strong HCO_3^- preference in *E. zodiacus* and *S. costatum* (Figs. 5 and 6a), are consistent with previous findings and provide, even though the novel role of eCA yet needs to be rigorously tested, further support for such a C_i recycling mechanism to operate in a large number of diatoms.

The role of intracellular CA is also under debate and its function(s) possibly differs strongly depending on the location within the cell (Badger and Price, 1994; Sültemeyer, 1998; Badger, 2003; Moroney and Ynalvez, 2007). This is important to bear in mind because the *in vivo* approach applied in this study (Palmqvist et al., 1994) does not differentiate between the various iCA forms. Furthermore, the estimates of the iCA activities rely on the diffusive influx of doubly labelled CO_2 and thus on membrane properties, intracellular pH and CO_2 concentrations as well as cell size and shape. Consequently, Δ values have arbitrary units and a direct species comparison should be treated with caution. In the present study, all four diatom species contained iCA regardless of the growth condition (Fig. 6b). In contrast to Burkhardt et al. (2001) who found a gradual increase in iCA activity with decreasing pCO_2 in the acclimation, results of our previous investigations (Fig. 6b) (Palmqvist et al., 1994; Rost et al., 2003; Trimborn et al., 2008) could not support this finding. Trimborn et al. (2008) suggested that cytosolic iCA may most likely be involved in a mechanism reducing the efflux from the cell. Consequently, species predominantly relying on HCO_3^- would have low cytosolic iCA activities to prevent the HCO_3^- taken up from being converted to CO_2. In contrast, species predominantly taking up CO_2 would have rather high cytosolic iCA activities to equilibrate CO_2 quickly into HCO_3^- and thus preventing it from leaking out of the cell. As shown in Fig. 6b, values for iCA activities were similar irrespective of the preferred carbon source (Fig. 5). Hence, the present data do not support the proposed CO_2 trapping mechanism by Trimborn et al. (2008). However, considering the methodological uncertainties about absolute activities and location of iCA, other approaches have to be applied to clarify the role of iCA in carbon acquisition.

4.4. The role of C_4-like photosynthesis in marine diatoms

Evidence for unicellular C_4-like photosynthesis came from ^{14}C-labelling experiments (Reinfelder et al., 2000; Morel et al., 2002) and experiments with a PEPC inhibitor for the marine diatom *T. weissflogii* (Reinfelder et al., 2004). Reinfelder et al. (2000) suggested that PEPC is the primary carboxylase in the cytoplasm that forms C_4 compounds from PEP and HCO_3^-. The C_4 compound malate/oxaloacetate is then transported into the chloroplast and decarboxylated by phosphoenol-pyruvate carboxykinase (PEPCK) in close proximity of RubisCO to support carbon fixation. Reinfelder et al. (2000) demonstrated that PEPC activity was up-regulated at low CO_2 concentrations in *T. weissflogii* and that the measured PEPC activities contributed up to 50% to carbon fixation under zinc limitation. Even though the assay applied in their study does not exclude the anaplerotic role of PEPC, which is considered to be involved in the synthesis of amino-acid precursors (Descolas-Gros and Oriol, 1992), the observation that the ^{14}C labelled C_4 compound malate was so rapidly formed in *T. weissflogii* (Reinfelder et al., 2000; Morel et al., 2002; McGinn and Morel, 2008) indicates photosynthetic C_4 fixation rather than anaplerotic processes. However, recent studies (e.g. Johnston et al., 2001; Granum et al., 2005; Kroth et al., 2008) criticized the findings by Reinfelder and others and have also provided evidence of C_3–C_4 intermediate photosynthesis in *T. weissflogii* (Roberts et al., 2007a,b).

In the current study, we used the same experimental ^{14}C-based assay as Reinfelder et al. (2000). According to Cassar and Laws (2007), the latter protocol provides higher PEPC activities than the Descolas-Gros and Oriol (1992) methodology. Even though the obtained results from the applied assays provide information on the *in vitro* and not on the *in vivo* activities, it is emphasized here that observed changes in the enzyme activities can be taken as relative changes in response to changes in pCO_2. In our experiments, the PEPC/RubisCO ratios indicate PEPC activities being generally lower than 3% relative to carbon fixation by RubisCO (Fig. 7). In comparison, similarly low values are typical for higher C_3 plants while much higher PEPC/RubisCO ratios (>20%) are indicative for the operation of the C_4 pathway (Keeley, 1999). Moreover,

the PEPC/RubisCO ratio did not increase with decreasing pCO_2 in any of the tested diatom species. Our low PEPC/RubisCO ratios are consistent with values obtained in laboratory experiments with *P. tricornutum* (Cassar and Laws, 2007) and in field studies with diatom-dominated phytoplankton assemblages (Tortell et al., 2006). The lack of significant PEPC activity in *T. pseudonana* (Fig. 7) is in agreement with the findings by Granum et al. (2005) and Roberts et al. (2007b). Granum et al. (2005) revealed the same levels of PEPC expression in *T. pseudonana* cells grown at 400 and 100 µatm pCO_2 using qPCR. Roberts et al. (2007b) demonstrated that *T. pseudonana* exclusively relies on C_3 photosynthesis even under low CO_2 concentrations either by performing ^{14}C short-term incubations as well as by measuring gene transcripts and protein abundances of C_4-metabolic enzymes. McGinn and Morel (2008) postulated the prevalence of a C_4-like pathway in *T. pseudonana* and *P. tricornutum* based on analysis of gene transcripts of PEPC and PEPCK and inhibitor studies of these enzymes. They observed a 3-fold upregulation of PEPC transcripts in *T. pseudonana* under low pCO_2 acclimation, but did not analyse total protein content for this enzyme. Please note that transcript levels are often not a reliable proxy for the amounts of corresponding functional enzymes (Gibon et al., 2004). Moreover, the localization of malate and/or oxaloacetate transporters to plastid membranes is not supported in *T. pseudonana* and *P. tricornutum* (Kroth et al., 2008), thus calling into question the importance of PEPC in C_4 fixation. Overall, the results of the present study suggest that PEPC activity does not significantly contribute to photosynthesis in the investigated species even under low CO_2 supply. In agreement with previous investigations, the combined data suggest rather an anaplerotic role of PEPC. Future experiments should explore whether or not other enzymes involved in C_4 photosynthesis fulfil the role that has previously been attributed to PEPC (Reinfelder et al., 2000, 2004).

Isotopic composition of autotrophs reflects changes in carbon fluxes as well as carbon assimilation pathways. Even though it is not possible to distinguish between C_4 photosynthesis and a classical CCM only on the basis of C isotope fractionation, the ^{13}C signal can provide some information about photosynthetic pathways. Opposed to the classical C_3 photosynthesis driven by RubisCO, the C_4-pathway is known to deplete the apparent fractionation. Most of this is the result of PEPC, which has a much lower intrinsic fractionation than RubisCO and uses HCO_3^- as its carbon source. The intrinsic fractionation factor of PEPC with respect to its substrate HCO_3^- is very small (~2.9 ‰, O'Leary et al., 1992) and when expressed relative to CO_2 leads to fractionation values of -4.7‰. In contrast, the intrinsic fractionation by RubisCO is very high with values ~29‰ (Raven and Johnston, 1991). If a large part of C_i was assimilated via PEPC prior to the fixation by RubisCO, this would lead to ε_p values be even negative. In our four diatoms, ε_p values ranged between 9‰ and 16‰ (Fig. 8). These ε_p values are in agreement with previous studies investigating fractionation in diatoms (Burkhardt et al., 1999; Cassar and Laws, 2007). We conclude that the observed ε_p values and the variation in response to the CO_2 supply can easily be explained by the operation of a classical CCM in the investigated species without invoking C_4 photosynthesis (e.g. Raven and Johnston, 1991; Rost et al., 2002; Trimborn et al., 2008).

According to Reinfelder et al. (2000, 2004) the operation of a C_4-like photosynthetic pathway provides a mean to significantly enhance the photosynthetic capacity under low CO_2 concentrations. However, when species assumed operating C_3 and C_4 metabolism are compared, we cannot observe the suggested advantage for the latter pathway. *T. pseudonana*, which appears to operate C_3 metabolism (Granum et al., 2005; Roberts et al., 2007a,b; present study), photosynthesizes as efficiently as *T. weissflogii* (Fielding et al., 1998; Burkhardt et al., 2001; S. Trimborn, unpublished data), for which C_4 metabolism has been postulated (Reinfelder et al., 2000, 2004; Morel et al., 2002). This is indicated by the similarly low $K_{1/2}$ (CO_2) for photosynthesis under low CO_2 supply (150 µatm pCO_2) being ~1.5 µmol L^{-1} CO_2 (Fielding et al., 1998; Burkhardt et al., 2001; S. Trimborn, unpublished data). Hence, even if the C_4 pathway plays a primary role in photosynthesis in some

species, it appears to provide no competitive advantage over diatoms operating classical CCMs.

4.5. Ecological implications and conclusions

It has been proposed that the dominance of species during bloom situations may depend on their ability to operate an efficient and regulated CCM (Rost et al., 2003; Trimborn et al., 2008). Therefore, one may assume that bloom-forming species possess most efficient and strongly regulated CCMs that allow to maintain high growth rates even under low CO_2 availability (e.g. Hobson, 1988; Rost et al., 2003) while non-bloom-forming species may not depend on such high growth rates and consequently C_i uptake rates. In the current study, the comparison of bloom-forming and non-bloom-forming diatoms revealed that all tested species had highly efficient CCMs (Table 2). In comparison with *T. pseudonana* and *E. zodiacus*, the two bloom-forming species *T. nitzschioides* and *S. costatum* showed strongly regulated CCMs (Table 2). Even though $K_{1/2}$ values for photosynthesis did not change significantly in *E. zodiacus*, significant changes in the C_i uptake systems and eCA activities were found when this species was acclimated to ambient and high pCO_2 levels, indicating strong regulation capacities of individual components of its CCM (Figs. 1–6, Table 2). It should be pointed out that significantly lower $K_{1/2}$ values for photosynthesis in *T. pseudonana* were obtained when exposed to even lower pCO_2 levels than the ones applied in our study (Fielding et al., 1998). This is consistent to additional data for *T. pseudonana* where C_i flux measurements revealed $K_{1/2}$ values for photosynthesis as low as ~120 µmol DIC L^{-1} for cells having been acclimated to 150 µatm pCO_2 (S. Trimborn, unpublished data). Furthermore, up-regulation of the CCM in response to low pCO_2 levels was also observed for non-bloom-forming species such as *T. weissflogii*, *Nitzschia navis-varingica*, and *Stellarima stellaris* (Burkhardt et al., 2001; Trimborn et al., 2008). Hence, the ability to operate an efficient and regulated CCM applies to bloom-forming as well as to non-bloom-forming diatoms. Furthermore, considering that the bloom-forming coccolithophore *Emiliania huxleyi* operates a rather inefficient CCM, but yet regulated CCM in response to changes in CO_2 (Rost et al., 2003), it can be concluded that an efficient CCM is not a prerequisite for bloom-forming species.

Taking into account that all diatom species examined so far mainly thrive in coastal areas, reasons for the observed high degree in CCM regulation of the investigated diatoms might be partially due to their occurrence in coastal areas that display regular and large changes in CO_2 levels (Hansen, 2002; Hinga, 2002) as well as highly variable light conditions (MacIntyre et al., 2000). Oceanic species, on the other hand, might exhibit less regulatory CCM capacities, but more studies are required to ultimately answer these questions. Future studies should also focus on the aspect of resource limitation in combination with CO_2 effects as species might respond differently under these conditions.

In view of the ongoing acidification of the oceans (Wolf-Gladrow et al., 1999; Orr et al., 2005; IPCC, 2007), the expected increase in aquatic pCO_2 may cause a down-regulation of the CCM capacity of diatoms (Figs. 1–4, 6, Table 2). This may result from an increasing diffusive CO_2 uptake and/or reduced energetic costs of the CCM. The latter can be ascribed to a decrease in leakage owing to a smaller outward CO_2 gradient under elevated pCO_2 (e.g. Raven and Lucas, 1985; Rost et al., 2006a,b). As a consequence, diatoms may optimize their resource allocation and thus have more energy available for carbon fixation.

Considering the low $K_{1/2}$ (CO_2) values for photosynthesis in the present and other studies focusing on marine diatoms (e.g. Burkhardt et al., 2001; Rost et al., 2003; Trimborn et al., 2008, present study), photosynthetic carbon fixation rates are close to saturation (~80–95%) in most diatom species under the projected high CO_2 levels. Large diatoms such as *S. stellaris* may benefit to a larger extent from the projected increase in CO_2 because of their lower affinities ($K_{1/2}$ (CO_2) of 7.4 µmol CO_2 L^{-1} at high pCO_2, Trimborn et al., 2008). It should be noted, however, that the observed $K_{1/2}$ values for photosynthesis were

obtained under a constant pH of 8.0. In the assays, the ratio of CO_2 to DIC therefore remains constant while in natural seawater an increase in CO_2 is associated with decreasing pH and corresponding changes in the CO_2 to DIC ratio. Nevertheless, incubations in unbuffered waters have also yielded higher photosynthetic carbon fixation rates under elevated pCO_2 for instance in laboratory experiments with *S. costatum* (Burkhardt and Riebesell, 1997). The projected CO_2/pH-related changes in seawater carbonate chemistry are likely to induce a species shift within the diverse group of diatoms, which may have consequences for the operation of the biological pump and thus for oceanic feedbacks to rising atmospheric CO_2.

References

Armbrust, E.V., Berges, J.A., Bowler, C., Green, B.R., Martinez, D., Putnam, N.H., Zhou, S., Allen, A.E., Apt, K.E., Bechner, M., Brzezinski, M.A., Chaal, B.K., Chiovetti, A., Davids, A.K., Demarest, M.S., Detter, J.D., Glavina, T., Goodstein, D., Hadi, M.Z., Hellsten, U., Hildebrand, M., Jenkins, B.D., Jurka, J., Kapitonov, V.V., Kröger, N., Lau, W.W.Y., Lane, T.D., Larimer, F.W., Lippmeier, J.C., Lucas, S., Medina, M., Montsant, A., Obornik, M., Parker, M.S., Palenik, B., Pazour, G.J., Richardson, P.M., Rynearson, T.A., Saito, M.A., Schwartz, D.C., Thamatrakoln, K., Valentin, K., Vardi, A., Wilkerson, F.P., Rokhsar, D.S., 2004. The genome of the diatom *Thalassiosira pseudonana*: ecology, evolution and metabolism. Science 306, 79–86.

Asmus, R., 1982. Field measurements on seasonal variation of the activity of primary producers on a sandy tidal flat in the northern Wadden Sea. Neth. J. Sea Res. 16, 389–402.

Badger, M.R., 2003. The role of carbonic anhydrases in photosynthetic CO_2 concentrating mechanisms. Photosynth. Res. 77, 83–94.

Badger, M.R., Price, G.D., 1989. Carbonic anhydrase activity associated with the cyanobacterium *Synechococcus* PCC7942. Plant Physiol. 89, 51–60.

Badger, M.R., Price, G.D., 1994. The role of carbonic anhydrase in photosynthesis. Annu. Rev. Plant Physiol. Plant Mol. Biol. 45, 369–392.

Badger, M.R., Palmqvist, K., Yu, J.-W., 1994. Measurement of CO_2 and HCO_3^- fluxes in cyanobacteria and microalgae during steady-state photosynthesis. Physiol. Plant. 90, 529–536.

Badger, M.R., Andrews, T.J., Whitney, S.M., Ludwig, M., Yellowlees, D.C., Leggat, W., Price, G.D., 1998. The diversity and coevolution of RubisCO, plastids, pyrenoids, and chloroplast-based CO_2-concentrating mechanisms in algae. Can. J. Bot. 76, 1052–1071.

Brewer, P.G., Bradshow, A.L., Williams, R.T., 1986. Measurement of total carbon dioxide and alkalinity in the North Atlantic Ocean in 1981. In: Trabalka, J.R., Reichle, D.E. (Eds.), The Changing Carbon Cycle — a Global Analysis. Springer, New York, pp. 358–381.

Buesseler, K.O., 1998. The decoupling of production and particulate export in the surface ocean. Glob. Biogeochem. Cycles 12, 297–310.

Burkhardt, S., Riebesell, U., 1997. CO_2 availability affects elemental composition (C:N:P) of the marine diatom *Skeletonema costatum*. Mar. Ecol. Prog. Ser. 155, 67–76.

Burkhardt, S., Riebesell, U., Zondervan, I., 1999. Stable carbon isotope fractionation by marine phytoplankton in response to daylength, growth rate, and CO_2 availability. Mar. Ecol. Prog. Ser. 184, 31–41.

Burkhardt, S., Amoroso, G., Riebesell, U., Sültemeyer, D., 2001. CO_2 and HCO_3^- uptake in marine diatoms acclimated to different CO_2 concentrations. Limnol. Oceanogr. 46, 1378–1391.

Burns, B.D., Beardall, J., 1987. Utilization of inorganic carbon acquisition by marine microalgae. J. Exp. Mar. Biol. Ecol. 107, 75–86.

Cassar, N., Laws, E.A., 2007. Potential contribution of ß-carboxylases to photosynthetic carbon isotope fractionation in a marine diatom. Phycologia 46, 307–314.

Colman, B., Rotatore, C., 1995. Photosynthetic inorganic carbon uptake and accumulation in two marine diatoms. Plant Cell Environ. 18, 919–924.

Colman, B., Huertas, I.E., Bhatti, S., Dason, J.S., 2002. The diversity of inorganic carbon acquisition mechanisms in eukaryotic microalgae. Funct. Plant Biol. 29, 261–270.

Dason, J.S., Huertas, I.E., Colman, B., 2004. Source of inorganic carbon for photosynthesis in two marine dinoflagellates. J. Phycol. 40, 285–292.

Descolas-Gros, C., Oriol, L., 1992. Variations in carboxylase activity in marine phytoplankton cultures. ß-carboxylation in carbon flux studies. Mar. Ecol. Prog. Ser. 85, 163–169.

Dickson, A.G., Millero, F.J., 1987. A comparison of the equilibrium constants for the dissociation of carbonic acid in seawater media. Deep-Sea Res. 34, 1733–1743.

Edwards, M., Licandro, P., John, A.W.G., Johns, D.G., 2005. Ecological status report: results from the CPR survey 2003/2004. SAHFOS Technical Report, vol. 2, pp. 1–6.

Elzenga, J.T.M., Prins, H.B.A., Stefels, J., 2000. The role of extracellular carbonic anhydrase activity in inorganic carbon utilization of *Phaeocystis globosa* (Prymnesiophyceae): a comparison with other marine algae using the isotope disequilibrium technique. Limnol. Oceanogr. 45, 372–380.

Falkowski, P.G., Katz, M.E., Knoll, A.H., Quigg, A., Raven, J.A., Schofield, O., Taylor, F.J.R., 2004. The evolution of modern eukaryotic phytoplankton. Science 305, 354–360.

Fielding, A.S., Turpin, D.H., Guy, R.D., Calvert, S.E., Crawford, D.W., Harrison, P.J., 1998. Influence of the carbon concentrating mechanism on carbon isotope discrimination by the marine diatom *Thalassiosira pseudonana*. Can. J. Bot. 76, 1098–1103.

Freeman, K.H., Hayes, J.M., 1992. Fractionation of carbon isotopes by phytoplankton and estimates of ancient CO_2 levels. Glob. Biogeochem. Cycles 6, 185–198.

Gibon, Y., Blaesing, O.E., Hannemann, J., Carillo, P., Höhne, M., Hendriks, J.H.M., Palacios, N., Cross, J., Selbig, J., Stitt, M., 2004. A robot-based platform to measure multiple enzyme activities in *Arabidopsis* using a set of cycling assays: comparison of changes in enzyme activities and transcript levels during diurnal cycles and in prolonged darkness. Plant Cell 16, 3304–3325.

Giordano, M., Beardall, J., Raven, J.A., 2005. CO_2 concentrating mechanisms in algae: mechanisms, environmental modulation, and evolution. Annu. Rev. Plant Biol. 56, 99–131.

Gran, G., 1952. Determinations of the equivalence point in potentiometric titrations of seawater with hydrochloric acid. Oceanol. Acta 5, 209–218.

Granum, E., Raven, J.A., Leegood, R.C., 2005. How do marine diatoms fix 10 billion tonnes of inorganic carbon per year? Can. J. Bot. 83, 898–908.

Guillard, R.R.L., Ryther, J.H., 1962. Studies of marine planktonic diatoms. Can. J. Microbiol. 8, 229–239.

Hansen, P.J., 2002. Effect of high pH on the growth and survival of marine phytoplankton: implications for species succession. Aquat. Microb. Ecol. 28, 279–288.

Hinga, K.R., 2002. Effects of pH on coastal marine phytoplankton. Mar. Ecol. Prog. Ser. 238, 281–300.

Hobson, L.A., 1988. Paradox of the phytoplankton — an overview. Biol. Oceanogr. 6, 493–504.

Hobson, L.A., McQuoid, M.R., 1997. Temporal variations among planktonic diatom assemblages in a turbulent environment of the southern Strait of Georgia, British Columbia, Canada. Mar. Ecol. Prog. Ser. 150, 263–274.

IPCC (Intergovernmental panel on climate change), 2007. Working Group 1 Report, The Physical Science Basis. http://ipcc-wg1.ucar.edu/wg1/wg1-report.html.

Johnston, A.M., Raven, J.A., Beardall, J., Leegood, R.C., 2001. Photosynthesis in a marine diatom. Nature 412, 40–41.

Keeley, J.E., 1999. Photosynthetic pathway diversity in a seasonal pool community. Funct. Ecol. 13, 106–118.

Korb, R.E., Saville, P.J., Johnston, A.M., Raven, J.A., 1997. Sources for inorganic carbon for photosynthesis by three marine species of marine diatom. J. Phycol. 33, 433–444.

Kroth, P.G., Chiovitti, A., Gruber, A., Martin-Jezequel, V., Mock, T., Parker, M. Schnitzler, Stanley, M.S., Kaplan, A., Caron, L., Weber, T., Maheswari, U., Armbrust, E.V., Bowler, C., 2008. A model for carbohydrate metabolism in the diatom *Phaeodactylum tricornutum* deduced from comparative whole genome analysis. PLoS ONE 3 (1), e1426. doi: 10.1371/ journal.pone.0001426.

Leggat, W., Badger, M.R., Yellowlees, D., 1999. Evidence for an inorganic carbon-concentrating mechanism in the symbiotic dinoflagellate *Symbiodinium* sp. Plant Physiol. 121, 1247–1255.

Lewis, E., Wallace, D.W.R., 1998. Program developed for CO_2 system calculations. ORNL/ CDIAC-105. Carbon Dioxide Information Analysis Center. Oak Ridge National Laboratory, U.S. Department of Energy.

MacIntyre, H.L., Geider, R.J., 1996. Regulation of RubisCO activity and its potential effect on photosynthesis during mixing in a turbid estuary. Mar. Ecol. Prog. Ser. 144, 247–264.

MacIntyre, H.L., Sharkey, T.D., Geider, R.J., 1997. Activation and deactivation of ribulose-1,5-bisphosphate carboxylase/oxygenase (RubisCO) in three marine microalgae. Photosynth. Res. 51, 93–106.

MacIntyre, H.L., Kana, T.M., Geider, J.R., 2000. The effect of water motion on short-term rates of photosynthesis by marine phytoplankton. Trends Plant Sci. 5, 12–16.

Marshall, H.G., 1976. Phytoplankton distribution along the Eastern Coast of the USA. Part 1. Phytoplankton composition. Mar. Biol. 38, 81–89.

Marshall, H.G., 1978. Phytoplankton distribution along the Eastern Coast of the USA. Part 2. Seasonal assemblages north of Cape Hatteras, North Carolina. Mar. Biol. 45, 203–208.

Martin, C.L., Tortell, P.D., 2008. Bicarbonate transport and extracellular carbonic anhydrase in marine diatoms. Physiol. Plant 133, 106–116. doi: 10.1111/j.1399-3054.2008.01054.x.

McGinn, P.J., Morel, F.M.M., 2008. Expression and inhibition of the carboxylating and decarboxylating enzymes in the photosynthetic C_4 pathway of marine diatoms. Plant Physiol. 146, 300–309.

Mehrbach, C., Culberson, C., Hawley, J., Pytkovicz, R., 1973. Measurement of the apparent dissociation constants of carbonic acid in seawater at atmospheric pressure. Limnol. Oceanogr. 18, 897–907.

Mills, D.K., Wilkinson, M., 1986. Photosynthesis and light in estuarine benthic microalgae. Bot. Mar. 29, 125–129.

Mitchell, C., Beardall, J., 1996. Inorganic carbon uptake by an Antarctic sea-ice diatom, *Nitzschia frigida*. Polar Biol. 16, 95–99.

Mook, W.G., 1986. ^{13}C in atmospheric CO_2. Neth. J. Sea Res. 20, 211–223.

Morel, F.M.M., Cox, E.H., Kraepiel, A.M.L., Lane, T.W., Milligan, A.J., Schaperdoth, I., Reinfelder, J.A., Tortell, P.D., 2002. Acquisition of inorganic carbon by the marine diatom *Thalassiosira weissflogii*. Funct. Plant Biol. 29, 301–308.

Moroney, J.V., Ynalvez, R.A., 2007. Proposed carbon dioxide concentrating mechanism in *Chlamydomonas reinhardtii*. Eukaryotic Cell 6 (8), 1251–1259. doi: 10.1128/ EC.00064-07.

Nelson, D.M., Tréguer, P., Brzezinski, M.A., Leynaert, A., Quéginer, B., 1995. Production and dissolution of biogenic silica in the ocean: revised global estimates, comparison with regional data and relationship to biogenic sedimentation. Glob. Biogeochem. Cycles 9, 359–372.

Nimer, N.A., Iglesias-Rodriguez, M.D., Merrett, M.J., 1997. Bicarbonate utilization by marine phytoplankton species. J. Phycol. 33, 625–631.

Nimer, N.A., Brownlee, C., Merrett, M.J., 1999. Extracellular carbonic anhydrase facilitates carbon dioxide availability for photosynthesis in the marine dinoflagellate *Prorocentrum micans*. Plant Physiol. 120, 105–111.

O'Leary, M.H., Madhavan, S., Paneth, P., 1992. Physical and chemical basis of carbon isotope fractionation in plants. Plant Cell Environ. 15, 1099–1104.

Orr, J.C., Fabry, V.J., Aumont, O., Bopp, L., Doney, S.C., Feely, R.A., Gnanadesikan, A., Gruber, N., Ishida, A., Joos, F., Key, R.M., Lindsay, K., Maier-Reimer, E., Matear, R., Monfray, P., Mouchet, A., Najjar, R.G., Plattner, G.-K., Rodgers, K.B., Sabine, C.L., Sarmiento, J.L., Schlitzer, R., Slater, R.D., Totterdell, I.J., Weirig, M.-F., Yamanaka, Y., Yool, A., 2005. Anthropogenic ocean acidification over the twenty-first century and its impact on calcifying organisms. Nature 437, 681–686.

Palmqvist, K., Yu, J.-W., Badger, M.R., 1994. Carbonic anhydrase activity and inorganic carbon fluxes in low- and high-Ci cells of *Chlamydomonas reinhardtii* and *Scenedesmus obliquus*. Physiol. Plant. 90, 537–547.

Price, G.D., Badger, M.R., Woodger, F.J., Long, B.M., 2007. Advances in understanding the cyanobacterial CO_2-concentrating mechanism (CCM): functional components, Ci transporters, diversity, genetic regulation and prospects for engineering into plants. J. Exp. Bot 59, 1441–1461. doi: 10.1093/jxb/erm112.

Ratti, S., Giordano, M., Morse, D., 2007. CO_2-concentrating mechanisms of the potentially toxic dinoflagellate *Protoceratium reticulatum* (Dinophyceae, Gonyaulacales). J. Phycol. 43, 693–701.

Raven, J.A., 1997. The vacuole: a cost-benefit analysis. Adv. Bot. Res. 25, 59–86.

Raven, J.A., Lucas, W.J., 1985. Energy costs of carbon acquisition. In: Lucas, W.J., Berry, J.A. (Eds.), Inorganic Carbon Uptake by Aquatic Photosynthetic Organisms. American Society of Plant Physiologists, Rockville, MD, pp. 305–324.

Raven, J.A., Johnston, A.M., 1991. Mechanisms of inorganic carbon acquisition in marine phytoplankton and their implications for the use of other resources. Limnol. Oceanogr. 36, 1701–1714.

Reinfelder, J.R., Kraepiel, A.M.L., Morel, F.M.M., 2000. Unicellular C_4 photosynthesis in a marine diatom. Nature 407, 996–999.

Reinfelder, J.R., Milligan, A.J., Morel, F.M.M., 2004. The role of the C_4 pathway in carbon accumulation and fixation in a marine diatom. Plant Physiol. 135, 2106–2111.

Roberts, K., Granum, E., Leegood, R.C., Raven, J.A., 2007a. Carbon acquisition by diatoms. Photosynth. Res 93, 79–88. doi: 10.1007/s11120-007-9172-2.

Roberts, K., Granum, E., Leegood, R.C., Raven, J.A., 2007b. C3 and C4 pathways of photosynthetic carbon assimilation in marine diatoms are under genetic, not environmental, control. Plant Physiol. doi: 10.1104/pp.107.102616.

Rost, B., Zondervan, I., Riebesell, U., 2002. Light-dependant carbon isotope fractionation in the coccolithophorid *Emiliania huxleyi*. Limnol. Oceanogr. 47, 120–128.

Rost, B., Riebesell, U., Burkhardt, S., Sültemeyer, D., 2003. Carbon acquisition of bloomforming marine phytoplankton. Limnol. Oceanogr. 48, 55–67.

Rost, B., Richter, K.-U., Riebesell, U., Hansen, P.J., 2006a. Inorganic carbon acquisition in red tide dinoflagellates. Plant Cell Environ. 29, 810–822.

Rost, B., Riebesell, U., Sültemeyer, D., 2006b. Carbon acquisition of marine phytoplankton. Effect of photoperiod length. Limnol. Oceanogr. 51, 12–20.

Rost, B., Kranz, S., Richter, K.-U., Tortell, P., 2007. Isotope disequilibrium and mass spectrometric studies of inorganic carbon acquisition by phytoplankton. Limnol. Oceanogr. Methods 5, 328–337.

Rotatore, C., Colman, B., Kuzma, M., 1995. The active uptake of carbon dioxide by the marine diatoms *Phaeodactylum tricornutum* and *Cyclotella* sp. Plant Cell Environ. 18, 913–918.

Shibata, M., Ohkawa, H., Katoh, H., Shimoyama, M., Ogawa, T., 2002. Two CO_2 uptake systems in cyanobacteria: four systems for inorganic carbon acquisition in *Synechocystis* sp. strain PCC6803. Funct. Plant Biol. 29, 123–129.

Silverman, D.N., 1982. Carbonic anhydrase. Oxygen-18 exchange catalyzed by an enzyme with rate contributing proton-transfer steps. Methods Enzymol. 87, 732–752.

Smetacek, V., 1999. Diatoms and the ocean carbon cycle. Protist 150, 25–32.

Sültemeyer, D., 1998. Carbonic anhydrase in eukaryotic algae: characterization, regulation, and possible function during photosynthesis. Can. J. Bot. 76, 962–972.

Sültemeyer, D., Klughammer, B., Badger, M.R., Price, G.D., 1998. Fast induction of high affinity HCO_3^- transport in cyanobacteria. Plant Physiol. 116, 183–192.

Tortell, P.D., Martin, C.L., Corkum, M.E., 2006. Inorganic carbon uptake and intracellular assimilation by subarctic Pacific assemblages. Limnol. Oceanogr. 51, 2102–2110.

Tortell, P.D., Payne, C.D., Li, Y., Trimborn, S., Rost, B., Smith, W.O., Riesselman, C., Dunbar, R.B., Sedwick, P., DiTullio, G.R., 2008. The CO_2 sensitivity of Southern Ocean phytoplankton. Geophys. Res. Lett 35, L04605. doi: 10.1029/2007GL032583.

Trimborn, S., Lundholm, N., Thoms, S., Richter, K.-U., Krock, B., Hansen, P.J., Rost, B., 2008. Inorganic carbon acquisition in potentially toxic and non-toxic diatoms: the effect of pH-induced changes in the carbonate chemistry. Physiol. Plant 133, 92–105. doi: 10.1111/j.1399-3054.2007.01038.x.

Wolf-Gladrow, D.A., Riebesell, U., 1997. Diffusion and reaction in the vicinity of plankton: a refined model for inorganic carbon transport. Mar. Chem. 59, 17–34.

Wolf-Gladrow, D.A., Riebesell, U., Burkhardt, S., Bijma, J., 1999. Direct effects of CO_2 concentration on growth and isotopic composition of marine phytoplankton. Tellus 51, 461–476.

Wolfstein, K., Hartig, P., 1998. The photosynthetic light dispensation system: application to microphytobenthic primary production. Mar. Ecol. Prog. Ser. 166, 63–71.

Zeebe, R.E., Wolf-Gladrow, D.A., 2001. CO_2 in Seawater: Equilibrium, Kinetics, Isotopes. Elsevier Science, Amsterdam.

Zhang, J., Quay, P.D., Wilbur, D.O., 1995. Carbon isotope fractionation during gas–water exchange and dissolution of CO_2. Geochim. Cosmochim. Acta 59, 107–114. **[SS]**